Integrated Control of Individual Scalars to Regulate Profiles and Improve MHD Stability in Tokamaks

A. Pajares[1], E. Schuster[1], K. Thome[2], A. Welander[2], J. Barr[2], N. Eidietis[2], D. Humphreys[2]

[1] Lehigh University, Bethlehem, Pennsylvania 18015, USA, [2] General Atomics, San Diego, California, USA

E-mail: andres.pajares@lehigh.edu

What do we mean by: "Integrated Control of ..."?

- We mean that the components of a control architecture work in an **interconnected fashion**, rather than working as isolated elements

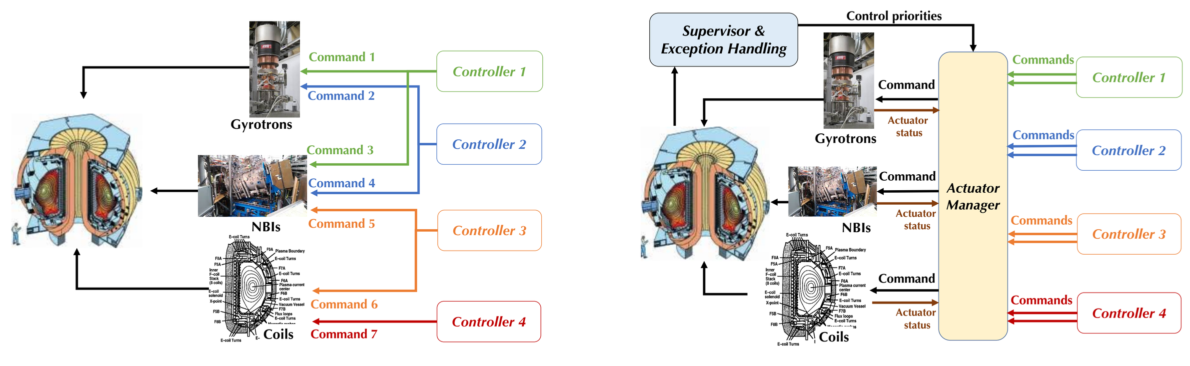

Non-integrated architecture **Integrated architecture**

In addition, an **integrated architecture** includes **supervisory and exception handling (S&EH) algorithms** and **actuator manager(s)** (more on this later)

What do we mean by: "Integrated Control of Individual Scalars to Regulate Profiles ..."?

- Controllability of a profile is sometimes limited. Instead, controlling associated scalars (e.g. volume-average) can be more attainable

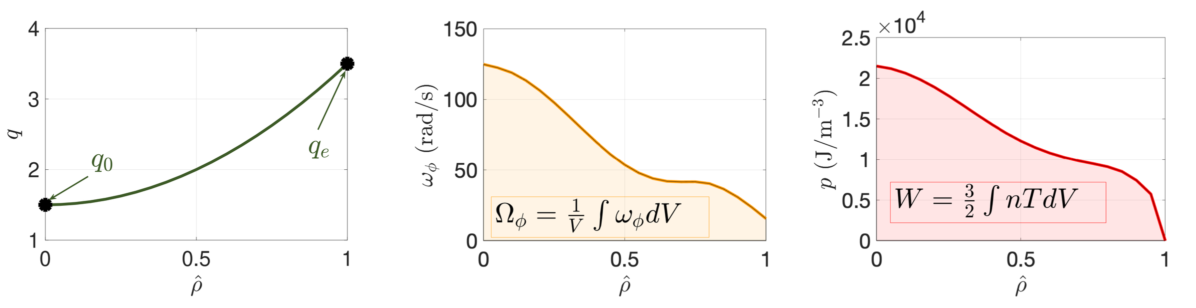

Current profile:

- Central safety factor, q_0
- Edge safety factor, q_e

Rotation profile:

- Volume-average rotation, Ω_ϕ

Pressure profile:

- Thermal stored energy, W

What do we mean by: "... Improve MHD Stability ..."?

- **Mode suppression by localized ECCD**, which is planned for ITER [1]

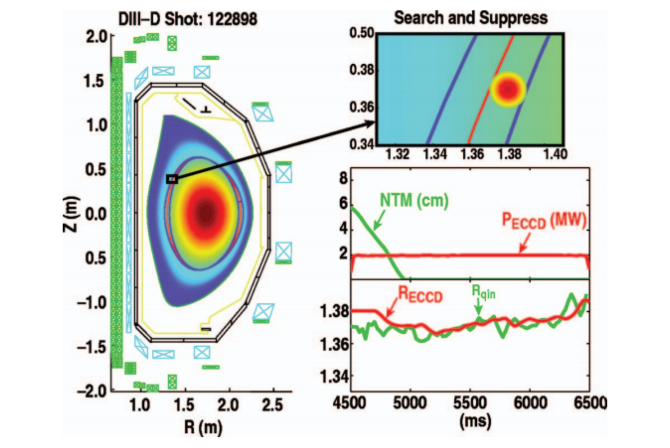

Figure source (used with permission): "Active control for stabilization of neoclassical tearing modes", by D. Humphreys et al, Phys. of Plasmas 13, 056113 (2006)

- Algorithms to track rational surface ($R_{q_{in}}$) with ECCD (R_{ECCD}) developed in DIII-D [2]
- May need additional NBI/EC heating to achieve "pre-NTM" values [3], which modify q_0, Ω_ϕ, and W $\Longrightarrow$ **NTM control coupled with scalars control**

[1] D. Humphreys et al., *Novel aspects of plasma control in ITER*, Physics of Plasmas 22, 021806 (2015)
[2] R. La Haye et al., *Control of neoclassical tearing modes in DIII-D*, Physics of Plasmas 9, 2051 (2002)
[3] S. Gunter et al., *Neoclassical tearing modes on ASDEX Upgrade: improved scaling laws, high confinement at high β_N and new stabilization experiments*, Nucl. Fusion 43, 161 (2003)

Summary of this Work: Test Integrated Architecture in DIII-D with Controllers + Actuator Manager + ONFR

- Actuators:
  - Gyrotrons
  - NBIs
  - E-coil
- Controllers:
  - Magnetics: q_0, q_e
  - Kinetics: W, Ω_ϕ
  - MHD: NTMs

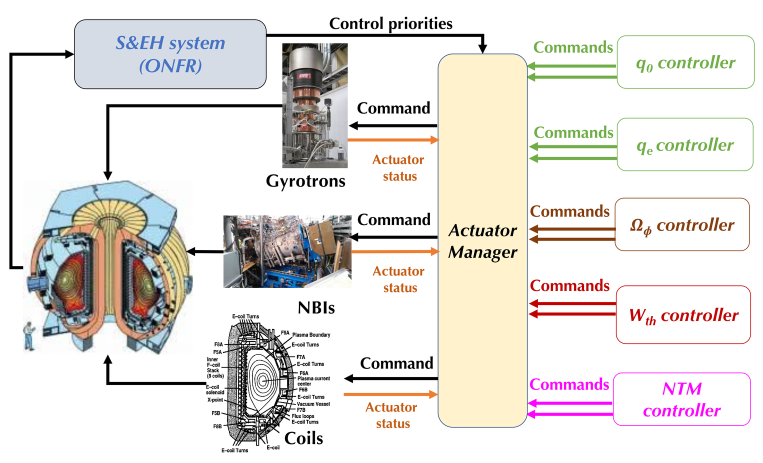

- **Actuator manager:** uses controller commands and control priorities to calculate **optimal actuator commands** within physical saturation limits
- S&EH: Off-Normal Fault Response (ONFR) [4]. Switches **control priorities** in real time (e.g. use gyrotrons for NTM control vs W_{th} control)

[4] N. Eidietis et al., *Implementing a finite-state off-normal and fault response system for disruption avoidance in tokamaks*, Nucl. Fusion 58, 056023 (2018)

Architecture has been Tested in Nonlinear Simulations using COTSIM (Control-Oriented Transport Simulator)

- COTSIM is a simulation code developed by the Lehigh University Plasma-Control Group [5] specially suited for control testing and tuning
- Employs **1D models for current, heat, and momentum transport**:

Magnetic diffusion equation: evolves poloidal flux Ψ

$$\frac{\partial \Psi}{\partial t} = \frac{\eta}{\mu_0 \rho_b^2 \hat{F}^2}\frac{1}{\hat{\rho}}\frac{\partial}{\partial \hat{\rho}}\left(\hat{\rho}\hat{F}\hat{G}\hat{H}\frac{\partial \Psi}{\partial \hat{\rho}}\right) + \eta \hat{H} 2\pi R_0 j_{ni}$$

- η: uses Spitzer-like model
- ρ_b, $\hat{F}$, $\hat{G}$, $\hat{H}$: 2D equilibrium factors
- j_{ni}: non-inductive current [6]

Electron heat-transport equation: evolves T_e

$$\frac{\partial\left(\frac{3}{2}n_e T_e\right)}{\partial t} = \frac{1}{\rho_b^2 \hat{H}}\frac{1}{\hat{\rho}}\frac{\partial}{\partial \hat{\rho}}\left(\hat{\rho}\frac{\hat{G}\hat{H}^2}{\hat{F}}n_e \chi_e \frac{\partial T_e}{\partial \hat{\rho}}\right) + Q_e$$

- χ_e: neoclassical + anomalous [7,8] (Bohm/gyro-Bohm, Coppi-Tang)
- Q_e: electron heating sources [5]

Toroidal momentum equation: evolves ω_ϕ

$$\frac{\partial (n_i \omega_\phi)}{\partial t} = \frac{1}{\bar{H}}\frac{1}{\hat{\rho}}\frac{\partial}{\partial \hat{\rho}}\left(\hat{\rho} n_i \bar{H}\langle r^2 (\nabla\hat{\rho})^2\rangle \chi_\phi \frac{\partial \omega_\phi}{\partial \hat{\rho}}\right) + t_w$$

- χ_ϕ: neoclassical + anomalous [7,8]
- $\bar{H}$, $\langle r^2(\nabla\hat{\rho})^2\rangle$: 2D equilibrium factors
- t_w: ion torque sources [5]

[5] Chapter 3 of *Integrated Control in Tokamaks using Nonlinear Robust Techniques and Actuator Sharing Strategies*, A. Pajares, 2019
[6] J. Barton et al, *Physics-based control-oriented modeling of the safety factor profile dynamics in high performance tokamak plasmas*, CDC, 2013
[7] M. Erba et al, *Validation of a new mixed Bohm/gyro-Bohm model for electron and ion heat transport against the ITER, Tore Supra and START database discharges*, Nucl. Fusion 38, 1013 (1998)
[8] W.M. Tang, *Microinstability-based model for anomalous thermal confinement in tokamaks*, Nucl. Fusion 26, 1605 (1986)

Architecture has been Tested in Nonlinear Simulations using COTSIM (Control-Oriented Transport Simulator)

- Employs **0D models** for the **pedestal** and **island-width evolutions**:

Analytical pedestal model: evolves temperature T_e^{ped} [9]

$$T_e^{ped} = \frac{\Delta}{2n}\frac{\alpha_c B_T^2}{2\mu_0 R q^2} \qquad \alpha_c = 0.8s\frac{1+\kappa_{95}^2(1+5\delta_{95}^2)}{2}$$

- Δ: pedestal width (predefined or from [9])
- α_c: max. normalized pressure gradient
- R, q, n, s: local values at pedestal top

Modified Rutherford equation: evolves island width w [10]

$$\frac{\tau_R}{w}\frac{dw}{dt} = \Delta_0' r + a_2 \frac{j_{BS}}{j_\phi}\frac{L_q}{w}\left[1 - \frac{w_{marg}^2}{3w^2} - K\frac{j_{EC}}{j_{BS}}\right]$$

- τ_R: island's resistive diffusion time
- Δ_0': classical stability index ($\approx -m$)
- a_2: geometric factor ($= 4$ for cylinder)
- j_{BS}, j_ϕ: local bootstrap and toroidal current
- L_q: normalized q-profile length
- w_{marg}: marginal island width ($\approx 2\sqrt{\epsilon}\rho_{\theta,i}$)
- j_{EC}, K: max EC current, alignment factor

- Employs **2D analytical solver** [11] for equilibrium reconstruction

[9] T. Onjun et al, *Models for the pedestal temperature at the edge of H-mode tokamak plasmas*, Physics of Plasmas 9, 5018 (2002)
[10] R. J. La Haye et al, *Higher stable beta by use of pre-emptive electron cyclotron current drive on DIII-D*, Nucl. Fusion 45, L37 (2005)
[11] J. Cerfon and J. P. Freidberg, *"One size fits all" analytic solutions to the Grad-Shafranov equation*, Physics of Plasmas 17, 032502 (2010)

Simulations Test Architecture in High-q_{min} Scenario to Achieve High Performance, NTM-Free Operation

- **Plasma 1:** simulated with **experimental inputs** from **shot 172538**
  - Except for reduced ECH, which results in **2/1 NTM development** at 2.7 s
- **Plasma 2:** simulated with **experimental inputs** from **shot 172538**
  - Except for slightly lower I_p (-0.05 MA)
  - Maximum ECH simulated, which results in **no NTM development**
- **Plasma 3:** simulated with **inputs determined in feedback**
  - The plasma starts from the conditions and inputs of the first simulation
  - The goal is to achieve the scalar evolutions of plasma 2 **using feedback**
  - The feedback scheme **does not know the required inputs for plasma 2**

Under Integrated Feedback (Turned On at 0.9 s), the Target Scalar Evolutions are Achieved in Simulations

Color code: Plasma 1 (no feedback), Plasma 2 (target), Plasma 3 (feedback: comes on at 0.9 s)

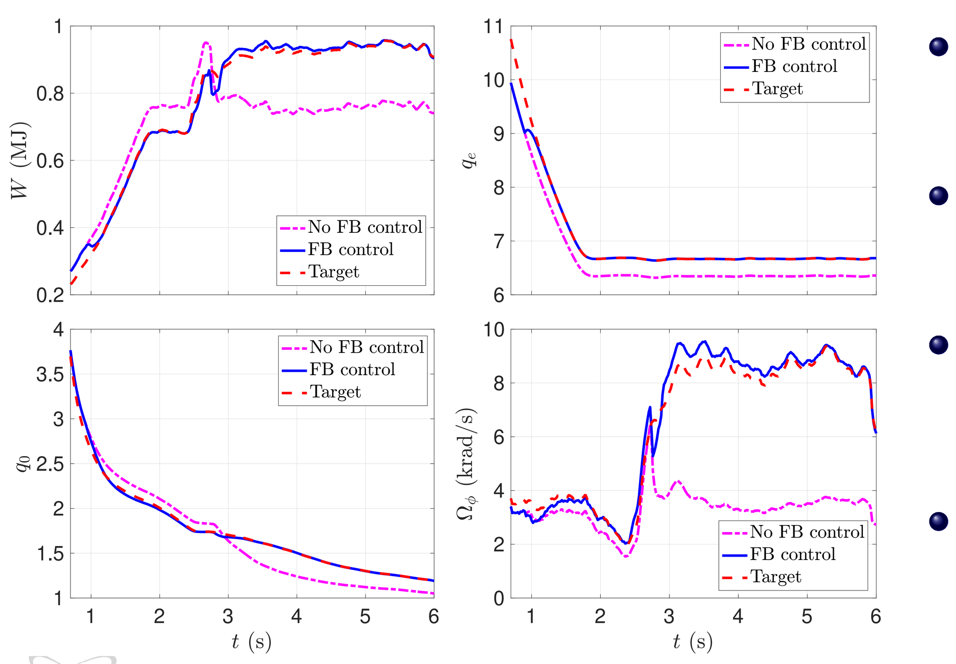

- W: decrease due to NTM development, recovery under feedback control
- q_e: control under feedback requires lower I_p values to elevate q_e
- q_0: control is slower in ramp-up but converges toward the end of the simulation
- Ω_ϕ: slight control loss after NTM development, recovery afterwards

NTM Suppression and the Inputs of the Target Plasma Simulation are Achieved under Feedback in Simulation

Color code: Plasma 1 (no feedback), Plasma 2 (target), Plasma 3 (feedback: comes on at 0.9 s)

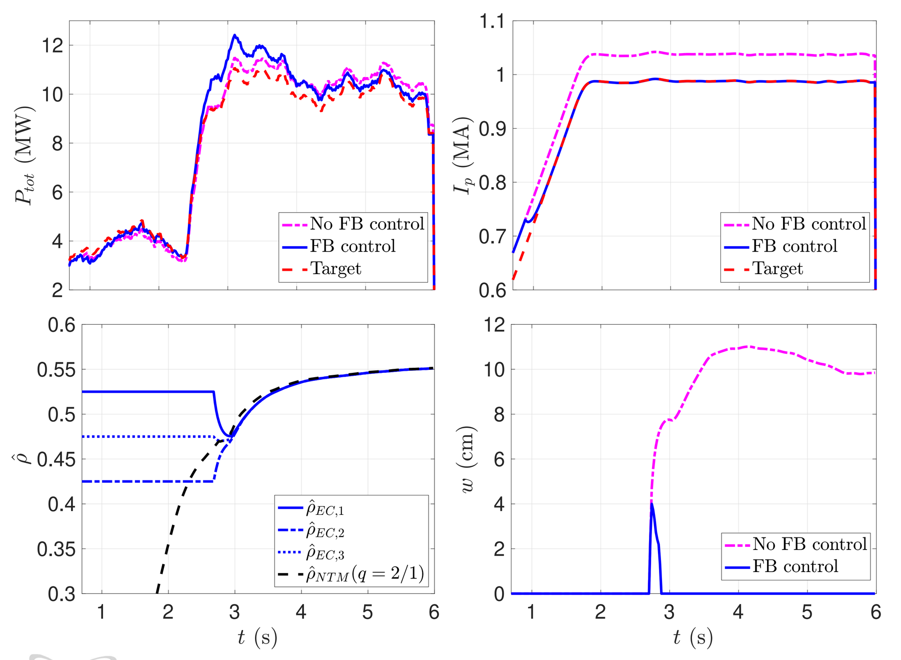

- Note: the feedback control does not have info about the red (target) inputs
- P_{tot}: higher under feedback during NTM development, down to target values later
- I_p: converges under feedback to target values
- $\hat{\rho}_{EC,i}$: steered toward $\hat{\rho}_{NTM}$ for NTM suppression ($t \geq 2.7$ s)
- w: saturates without feedback, but $\to 0$ with feedback

Experiments in DIII-D Test Architecture in High-q_{min} Scenario Following Similar Ideas as in Simulation

- **Plasma 1:** using **experimental inputs** similar to **shot 172538**
  - Except for reduced ECH ≤ 1 MW
- **Target:** evolutions far from Plasma 1, but attainable
  - Slightly lower I_p ($\approx$ -0.05 MA)
  - Ideally, **no NTM development**
- **Plasma 3: inputs determined in feedback**
  - The plasma starts from the inputs of the Plasma 1
  - The goal is to achieve the targets **using feedback**
  - The feedback scheme **does not know the required inputs for the target**

Feedback Architecture Tested in DIII-D (Turned On at 2 s) with less Actuation Capability than in Simulation

Color code: Plasma 1 (no feedback), Target, Plasma 3 (feedback: comes on at 2 s)

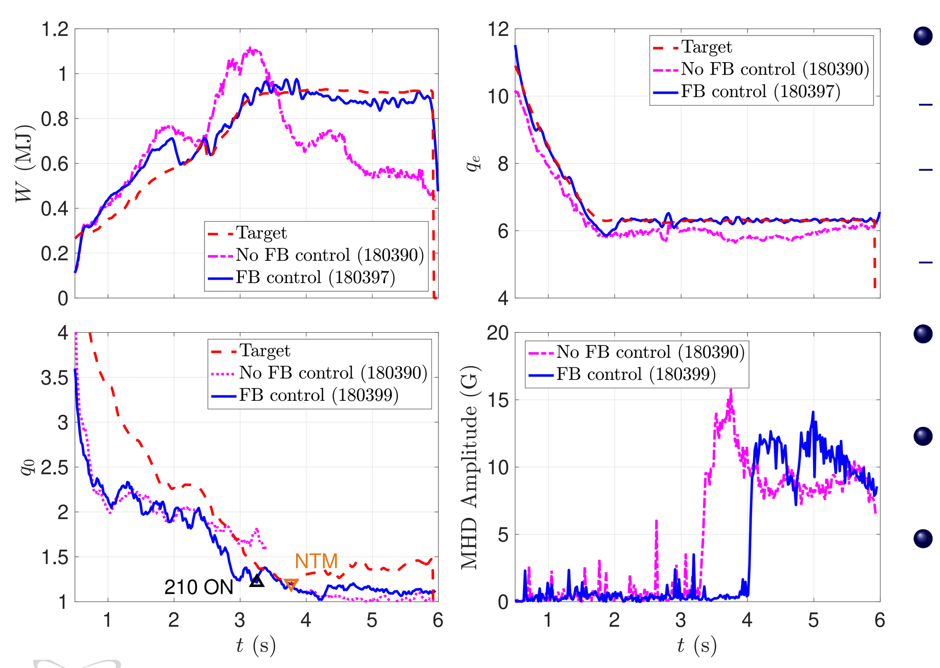

- Same scenario as in simulations, however:
  - No counter-I_p NBIs $\Longrightarrow$ no Ω_ϕ control
  - Limited off-axis NBIs (210 in 2 s pulse) $\Longrightarrow$ limited q_0 control
  - ECH ≤ 1.5 MW $\Longrightarrow$ no NTM suppression
- W + q_e: good regulation in feedback (turned on at $t \geq 2$ s)
- q_0: good regulation only if 210s on and until NTM shows up
- No NTM suppression, but a delay in its appearance is seen (due to W control)

FB Inputs Achieved Scalar Control and Delay in NTM Development, but No Significant NTM Suppression

Color code: Plasma 1 (no feedback), Plasma 3 (feedback: comes on at 2 s)

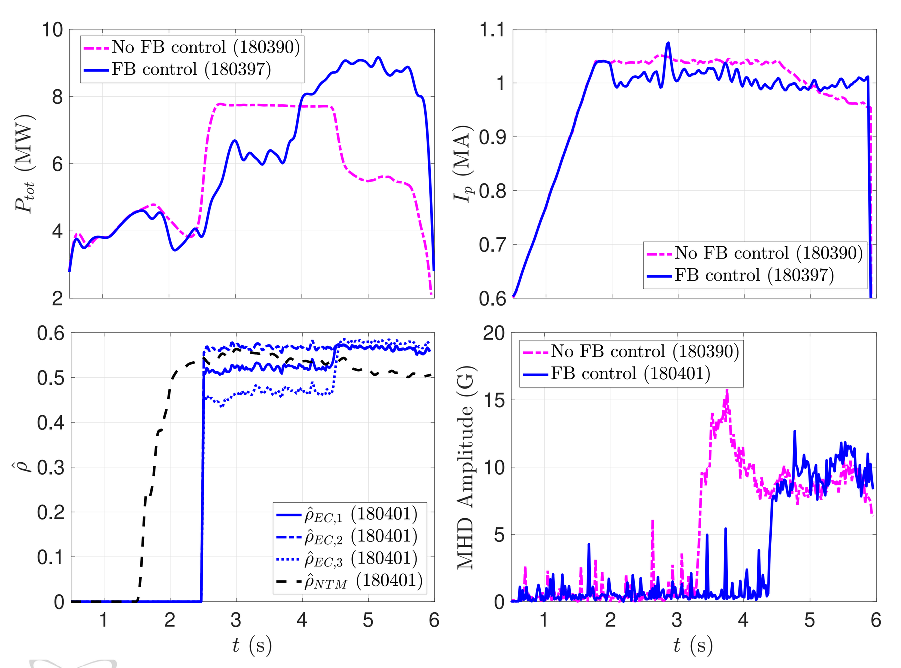

- P_{tot}: higher under feedback at $t \geq 4$ s due to NTM development
- I_p: regulated under feedback for q_e control, driven to lower value
- $\hat{\rho}_{EC,i}$: defective steering due to wrong settings within PCS ($t \geq 4.5$ s)
- No significant NTM suppression, but delay in NTM appearance (due to W control)

Conclusion & Future Work

- An **integrated-control architecture** has been **successfully developed** and implemented **in the DIII-D PCS**
  - **Preliminary** architecture $\Longrightarrow$ work needed to define final architecture
- It shows **good performance** in **simulations** and DIII-D **experiments**
  - This provides **initial validation** and encourages **further experimental tests**
- Future work may include:
  - Addition of **new actuators and controllers** (e.g. magnetic coils + shape control, gas puffing + pellet injectors + density control)
  - Integration of the architecture **with other elements of the DIII-D PCS** (e.g. integration with Proximity Control)
  - Testing in **ITER-like scenarios** using COTSIM

Appendix A: Actuator Manager Solves a Nonlinear, Constrained Optimization Problem in Real Time

The actuator commands $\mathbf{u}$ are calculated by solving the following problem,

$$\min_{\mathbf{u}} \underbrace{\mathbf{s}^T \mathbf{Q}\, \mathbf{s}}_{\text{Metric for controller-request status}} + \underbrace{\mathbf{u}^T R\, \mathbf{u}}_{\text{Metric for actuator use}}$$

subject to constraints

(1) **Controller requests:** $\underbrace{f(\mathbf{u})}_{\text{nonlinear function}} + \underbrace{\mathbf{s}}_{\text{slack variables}} = \underbrace{\mathbf{u}_{\mathbf{requests}}}_{\text{controller requests}}$

(2) **Actuation limits:** $\mathbf{u} \subset \underbrace{\mathcal{U}_{limits}}_{\text{Subset of feasible } \mathbf{u}}$

- Both $\mathbf{Q}$ and R prioritize **controller requests** and **actuators**, respectively
- The utility function $f(u)$ is defined by the controllers in use, characterizing the relative satisfaction of **competing priorities** as a numerical quantity
- Some linear examples of $f(u)$:
  - Total power $= \sum_i u_i$, Torque $= u_{\text{co-}I_p} - u_{\text{counter-}I_p}$, Actuator failure $= u_i$ ($= 0$)

Appendix B: Nonlinear Control Design for Catch-and-Subdue Power using Lyapunov Techniques

Island-width control with catch-and-subdue: start with the Modified Rutherford equation

$$\frac{\tau_R}{r}\frac{dw}{dt} = \Delta_0' r + a_2 \frac{j_{BS}}{j_\phi}\frac{L_q}{w}\left(1 - \frac{w_{marg}^2}{3w^2}\right) - \frac{a_2 L_q}{j_\phi}\Bigg[\underbrace{\sum_k \frac{K_{EC,k}}{w} j_{EC,k}(\hat{\rho}_k^{max})}_{\text{pre-emptive}} + \underbrace{\frac{K_{c\&s}}{w} j_{c\&s}(\hat{\rho}_{c\&s}^{max})}_{\text{catch-and-subdue}}\Bigg], \quad (1)$$

assume the power of the pre-emptive ECCD clusters is set to the maximum available. By setting

$$j_{c\&s}(\hat{\rho}_{c\&s}^{max}) = \frac{K_P \frac{w^2 \tau_R j_\phi}{r L_q} + j_{BS}}{K_{c\&s}}, \quad (2)$$

where $K_P > 0$ is a design parameter, (1) becomes

$$\frac{\tau_R}{r}\frac{dw}{dt} = \Delta_0' r - \frac{\tau_R}{r} a_2 K_p w - a_2 \frac{j_{BS}}{j_\phi}\frac{L_q}{w}\frac{w_{marg}^2}{3w^2} - \frac{a_2 L_q}{j_\phi}\sum_k \frac{K_{EC,k}}{w} j_{EC,k}(\hat{\rho}_k^{max}). \quad (3)$$

It is assumed that the pre-emptive clusters provide a stabilizing effect, so the last term in (3) is non-positive, and

$$\frac{dw}{dt} < -a_2 K_p w \implies w < w_0 e^{-t/\tau}, \quad (4)$$

where w_0 is the initial island width, and $\tau \triangleq 1/(a_2 K_p)$ is the characteristic suppression time. $P_{c\&s}^{req}$ is computed from (2) as

$$P_{c\&s}^{req} = \frac{1}{j_{c\&s}^{dep}(\hat{\rho}_{c\&s}^{max})}\left[\frac{n_e(\hat{\rho}_{c\&s}^{max})}{T_e(\hat{\rho}_{c\&s}^{max})}\frac{\frac{\tau_R}{r}\frac{K_P j_\phi}{L_q} w^2 + j_{BS}}{w\frac{F_{c\&s}}{\delta_{c\&s}^{w}} + K_{c\&s}} - \sum_k j_{EC,k}^{dep}(\hat{\rho}_k^{max}) P_{EC,k}\right]. \quad (5)$$